Supplementary Information

Improved thermal and oxidation stability of bis(triethoxysilyl)ethane (BTESE)-derived membranes and their gas permeation properties

Xin Yu, Hiroki Nagasawa, Masakoto Kanezashi and Toshinori Tsuru

--------------- Supplementary Information-1 (SI-1) ---------------

The time course of TG weight with firing temperature was studied and is shown in Figure SI 1. BTESE powders were fired from room temperature to 250 °C and kept for 1 h, then the temperature was increased to 400 °C. The TG weight was drastically decreased to around 200 °C due to the decomposition of NH_4Cl [X. Yu et al J. Membr. Sci., 511 (**2016**) 219-227], and then even BTESE powders calcinated at 250 °C remained stable for nearly 1 h, which confirmed the decomposition of NH_4Cl was completed at 250 °C.
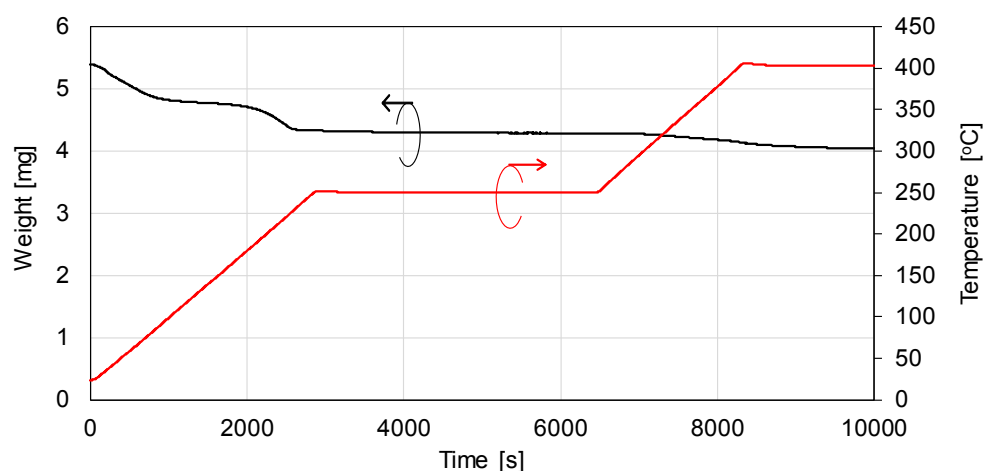

Figure SI-1. A time course of TG weight for BTESE-derived powders (H_2O ratio of 240, H^+ ratio of 0.01) fired in N_2 from room temperature to 400 °C with a ramping rate of 5 °C/min. Powders were kept at 250 °C for 1 h.

Figure SI2 shows the values for gas permeance of the intermediate layer, the top layer, and the total layers (total membrane) of a BTESE-derived membrane fired at 550 °C, which was used to calculate the gas-permeation resistance, as summarized in Figure SI3.

Many studies have applied resistance in a series model to explain the transport properties of membranes (Nagasawa et al., *J. Membr. Sci., 498* (2016) 336–344), and the resistance, R_i, is defined as: $$R_i = \frac{1}{P_i},$$ where P_i is the permeance. The total permeation resistance across the membrane, R, can be given as follows, $R = R_1 + R_2$, where R_1, R_2 are the permeation resistance of the SiO$_2$-ZrO$_2$ layer (including supports) and the BTESE-derived top layer.

The resistances of various gases permeating the intermediate layer and the total layers (total membrane) were calculated and appear in Figure R2. H$_2$ has a small diameter, and its resistance was 1.6×10^5, 5.1×10^5 and 6.7×10^5 (m^2 s Pa)/mol for the SiO$_2$-ZrO$_2$ layer (R_1), the top layer (R_2), and the total membrane (R), respectively, which indicated that the top layer (R_2) dominated 76% of the total permeation resistance (R). For gases with large diameters, such as CH$_4$ and CF$_4$, the percentages were 99.7% and 99.998%, respectively. As shown in Figure R1, the permeance of the top layer ($1/R_2$) was almost the same as the total separation membrane. This trend was the same for all membranes fired at 300, 550 and 700 °C.
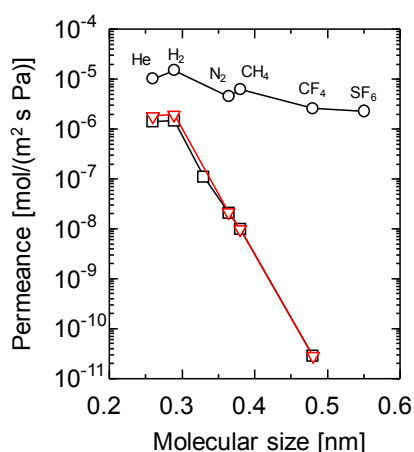

Figure SI 2. The relationship between gas permeance and kinetic diameter at 300 ℃ for a BTESE-derived membrane fired at 550 ℃. The circles, squares and triangles are the SiO$_2$-ZrO$_2$ layer, top layer and total membrane, respectively.
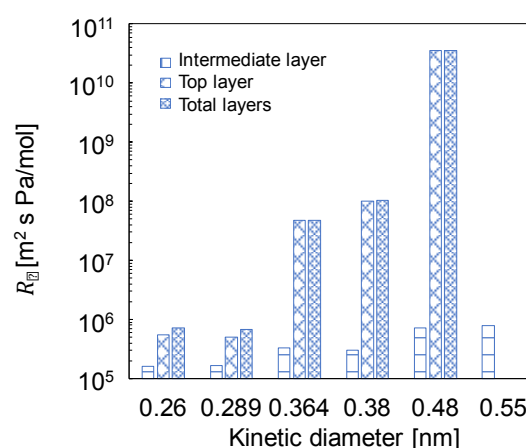

Figure SI 3. The relationship between R_i and kinetic diameter at 300 ℃ for the intermediate layer, top layer and total membrane.

The morphology of BTESE membrane was studied by examining cross-sectional SEM images and shown in Figure R4. The samples (a) and (b) were BTESE-derived membranes fired at 300 and 700 ℃, respectively. The particle layer was uniformly distributed with Al_2O_3 particles (0.2 µm), which could be clearly observed in both membranes. However, the membrane morphology showed no change even when the firing temperatures were increased. Regarding the thickness of the separation top layer, as we reported many times, the intermediate and separation layers were too thin to distinguish the thickness differences (X Yu et al., Journal of Membrane Science 511 (2016) 219–227).
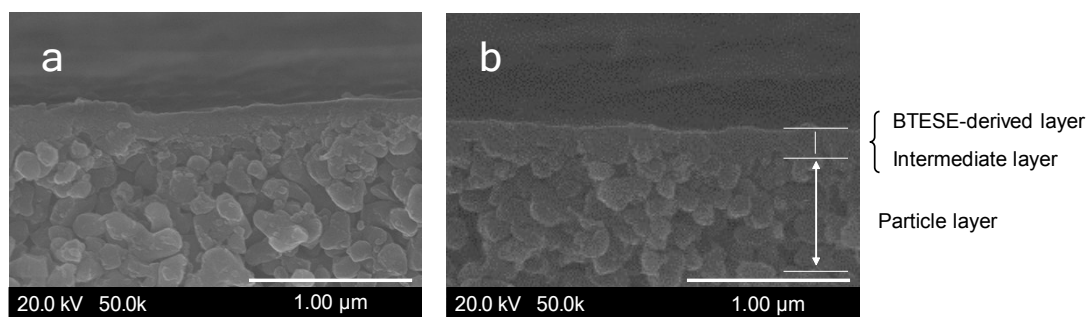

Figure SI4. The cross section of BTESE-derived membranes prepared at 300 (a) and 700 °C

Figure SI5 shows a schematic illustration of the BTESE-derived organosilica membranes calcined at 300, 550, and 700 °C. A proposed structure of silica after gelation shows the presence of three pore domains: small, intermediate, and larger pore sizes that are referred to as D_{small}, D_{int}, and D_{large}, as detected by PALS (Mikel C. Duke et al., Adv. Funct. Mater. 2008, 18, 3818–3826), or bimodal structures such as internal pores and unconnected pores as reported by Qi et al. (J. Mater. Chem. A, 2017, vol. 5, 24657-24666). Gas molecules with small-sized diameters such as He and H_2 can permeate connected pores, neck pores (or D_{small}), and unconnected pores (or D_{larger}), while gas molecules with large diameters such as N_2, CH_4, CF_4 and SF_6 can only permeate the unconnected pores. In addition, they concluded that both connected and unconnected pores were shrunken at high temperatures.

In this manuscript, BTESE-derived membranes were fired at 300, 550, and 700 °C, as shown in Figure SI5. N_2 can access the blue parts and the sizes of network pores and unconnected pores (larger pores) were decreased with higher firing temperatures. All the membranes showed H_2/CH_4 ratios higher than 60 since most of the pores were formed by networks that N_2 and CH_4 could not permeate.
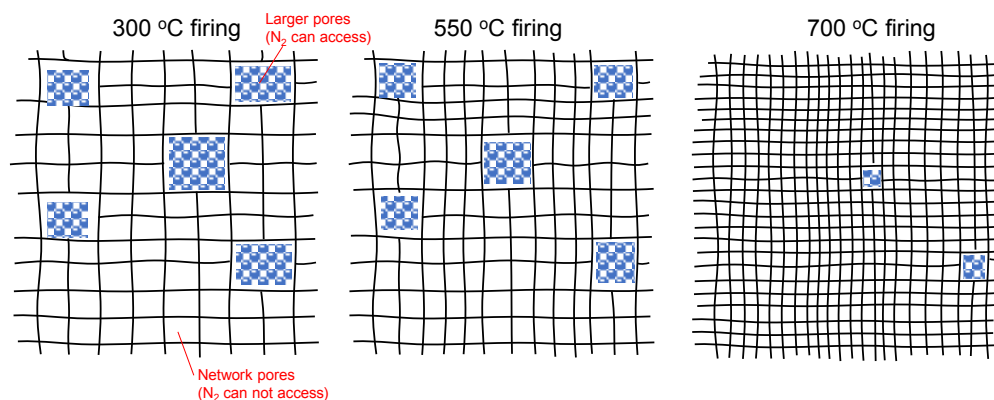

Figure SI5. Schematic illustration of the BTESE-derived organosilica membranes calcined at 300, 550, and 700 °C.

Table SI-1: The H_2 permeances and H_2/CH_4 selectivities for Figure 7.

	H_2 permeance mol/(m^2 s Pa)	H_2/CH_4 selectivity [-]	Ref.
BTESE 300 ºC	1.5E-06	32	
BTESE 300 ºC	1.0E-06	15	
BTESE 300 ºC	9.0E-07	62	
BTESE 300 ºC	7.5E-07	120	
BTESE 550 ºC	1.6E-06	93	
BTESE 550 ºC	6.1E-07	390	this work
BTESE 550 ºC	3.5E-07	89	
BTESE 550 ºC	1.5E-06	152	
BTESE 550 ºC	6.8E-07	80	
BTESE 700 ºC	6.7E-07	507	
BTESE 700 ºC	7.2E-07	920	
BTESE 700 ºC	5.4E-07	287	
ZIF-7	8.0E-08	6	48
ZIF-7	4.0E-07	10	49
ZIF-7	4.6E-08	15	47
ZIF-8	6.0E-08	13	49
ZIF-22	1.9E-07	5	49
ZIF-90	2.1E-07	19	49
ZIF-95	2.0E-06	11	49
ZIF-8	2.5E-07	23	50
Na-A-zeolite	6.9E-08	1200	45
Zeolite-T	1.7E-08	83	
	9.6E-09	48	46
	9.3E-09	47	
	9.6E-09	48	
Silica	5.0E-07	4000	9
	3.0E-07	1000	8
	4.0E-08	160	8
	1.0E-08	221	42
	1.0E-08	162	42
	4.7E-07	350	43
	5.1E-07	400	43
	5.2E-08	60	44
	6.8E-08	350	44